^{4}He Adsorbed on the Outer Surface of Carbon Nanotube Bundles

M. C. Gordillo

Departamento de Sistemas Físicos, Químicos y Naturales. Facultad de Ciencias Experimentales, Universidad Pablo de Olavide, Carretera de Utrera, km 1. 41013 Sevilla, Spain

(Received 9 May 2008; published 21 July 2008)

The results of diffusion Monte Carlo calculations on the behavior of ^{4}He adsorbed on the external surface of a bundle of carbon nanotubes are presented. The corrugation effects are found to be very important, making the outside part of the bundles a quite inhomogeneous substrate. No stable solid helium monolayer at high density was found. Instead, helium atoms are promoted to a second quasi-one-dimensional phase on top of the liquid first layer. On increasing the helium intake, a two layer structure is formed in which the helium directly in contact with the carbon surface solidifies.

DOI: 10.1103/PhysRevLett.101.046102 PACS numbers: 68.43.Bc, 61.48.De, 68.90.+g

Carbon nanotubes have been the subject of much work both theoretical and experimental since they were first described by Iijima in 1991 [1]. This has allowed the discovery of many interesting properties of these long and narrow cylinders, such as, for instance, the possibility of being used as gas adsorbents [2]. A carbon nanotube can admit species with the appropriate radius inside or on its external surface. If we have an isolated tube, that outer part is a cylindrical shell, but in the most common cases, what we have is a set of closed packed parallel tubes usually termed a bundle. This means that only the part of the cylindrical surface of the tubes located on the fringes of the bundle is accessible to the gas uptake. Since the nanotubes are usually synthesized as close capped structures, those external surfaces are the only adsorption sites unless the tubes are intentionally opened. The other possibility, the interchannels among every three tubes in the inner part of a bundle, seems to be forbidden [3,4].

In recent years, there has been some theoretical and experimental work on the adsorption on the accessible surface of a carbon nanotube bundle. Most of it is related to classical noble gases or small molecules [5–11], but there are some experiments about quantum gases on the same sites [12–21]. On the other hand, the only quantum calculations are of helium outside isolated carbon nanotubes [22,23] or a single atom or a small cluster in a groove [24,25]. The aim of this work is then to perform a full quantum Monte Carlo calculation on helium on the accessible surfaces of a bundle of (10,10) carbon nanotubes. The chosen technique was a Diffusion Monte Carlo (DMC) [26] calculation.

A fundamental ingredient of the DMC method is the so-called trial wave function. In principle, the DMC algorithm is able to correct the differences between the approximate trial and the real functions for a system of bosons if both are close enough. Any trial that takes into account all the physical information known *a priori* about the system under consideration should give an exact solution, specially if its parameters have been adjusted with a separate variational calculation. In our case, each helium phase has a different trial function. All of them have a common part given by

$$\Phi_J = \prod_{i<j} \exp\left[-\frac{1}{2}\left(\frac{b_{\text{He-He}}}{r_{ij}}\right)^5\right] \prod_i \exp\left[-\frac{1}{2}\left(\frac{b_{\text{C-He}}}{r_{\text{C-}i}}\right)^5\right] \tag{1}$$

which has a contribution for all the He-He pairs (first one), and for all the C-He ones (second part). In all cases, $b_{\text{He-He}} = 3.07$ Å (the standard value in many calculations) [26,27] and $b_{\text{C-He}} = 2.30$ Å (obtained variationally). The value of $b_{\text{C-He}}$ is an indication of the importance of carbon-helium corrugation effects. Then, depending on the phase we are considered, the trial is multiplied by one of the two following forms:

$$\Phi_1 = \prod_i \exp[-a_1(x - x_{\text{site}})^2 - a_1(y - y_{\text{site}})^2 - b_1(z - z_{\text{site}})^2] \tag{2}$$

or

$$\Phi_2 = \prod_i \exp[-a_2(r - r_{\text{center}})^2] \tag{3}$$

where all the parameters were obtained variationally for each phase and could be zero. In all cases, the standard deviations of the energies obtained for any phase were no greater than 0.1 K, indicating that all the trials are of good quality. The He-He potential was taken from Ref. [28] while the individual C-He interactions were assumed to be of the Lennard-Jones type and were taken from Ref. [29].

We started the study of the system by calculating the binding energy of a single ^{4}He atom on the groove in between two (10,10) carbon nanotubes. In this case, the simulation cell comprised only these two cylinders located parallel to each other and whose centers are separated by 17 Å in what is the x axis of the simulation cell, being the z coordinate parallel to the long axis of the tubes. In this case, as in the quasi-one-dimensional phase considered

below, the trial function was $\Phi_J\Phi_1$ with $b_1 = 0$ and $a_1 = 1.8$ Å^{-2}. x_{site} and y_{site} are the coordinates in which the ^{4}He binding potential was minimum for a smooth version of the C-He interaction, i.e., points located at 9.5 Å of both centers of the nanotubes. Since both nanotubes are corrugated, there is also some influence of the relative orientation of one cylinder to each other in the binding energy of helium in the resulting groove. That was taken into account, and the results of all the calculations are included in Fig. 1. The initial guess was to fix a cylinder and rotate the other clockwise. Then, we should get the same energy after rotating the second cylinder an angle of $2\pi/n$, being n the nanotube index, in our case, 10. The results are shown as a set of full squares joined by a dashed line in Fig. 1 (a guide to the eye). The rotation angle of the second cylinder to the fixed one is the quantity indicated in the x axis of the figure. However, that does not exhaust all the possibilities. In the maxima and minima of the dashed line of Fig. 1, we rotated the formerly fixed cylinder counterclockwise to see what happened to the binding energies. We also considered the displacement of the nanotubes with respect to each other in several orientations, an example of the values obtained being the crosses in the figure. The absolute maximum and minimum helium energies at 0 K after all these changes are indicated by two open squares and correspond to binding energies of 227.54 ± 0.01 and 201.85 ± 0.01 K, respectively. These compare favorably with the experimental results given in Ref. [13] (range between 210 and 250 K), and Ref. [17] (212 K, to be compared to our average of ~215 K). They also compare favorably with the calculations of Ref. [25], (~211 K in a similar simulation cell). That work includes also a reference to the influence of corrugation in the binding energy of ^{4}He in a groove. The energies in that case go from ~209 to ~220 K, a range similar to the one found here.

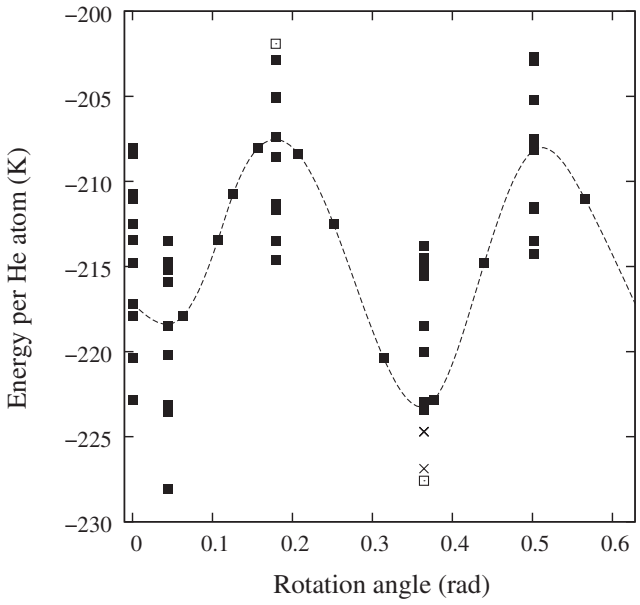

FIG. 1. Energy per helium atom in the infinity dilution limit (full squares). A dashed line joints the results obtaining by fixing the orientation of a cylinder and rotating the other one. Additional simulations were performed to see the influence of the rotation of the previously fixed cylinder in the binding energies. Crosses indicate what happens in two cases when the cylinders instead of being rotated are displaced slightly in the z direction. Open squares represent the maximum and minimum values of the ^{4}He the binding energies.

The first phase to appear is the quasi-one-dimensional one (quasi-1D), on the grooves in between two nanotubes. To study that, we used the same trial function and simulation cell than in the infinite dilution limit. The number of helium atoms was fixed to 30, and the appropriate length of the simulation cell was used. To afford an easy comparison, we subtracted the corresponding binding energies per particle (E_0's) in the infinite dilution limit, being those 227.54 ± 0.01 K (full squares, maximum binding energy), 201.85 ± 0.01 K (open squares, minimum binding energy), and 222.66 ± 0.01 K (open circles, an intermediate case). These three sets of calculations are fairly representative of all the simulations done. The results could be seen in Fig. 2. In most cases, we found a quasi-one-dimensional liquid, with very small energy per particle at zero pressure with respect to the infinite dilution limit (in our examples, 0.051 and 0.096 K, respectively), while the third case is fairly representative of a minority of systems and it is a gas. The system is a liquid or a gas depending on the corrugated structure of the groove, not on the binding energy. Since one expects different relative orientations of the tubes, the filling of the grooves would proceed from the more binding to the less binding ones up to completion. Such quasi-one-

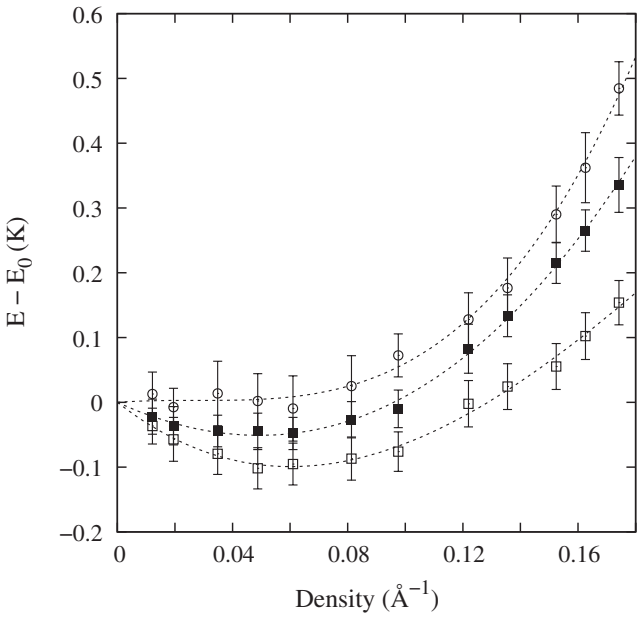

FIG. 2. Energy per helium atom for three representative cases of quasi-1D arrangements. In all cases, binding energies for the infinite dilution limit were subtracted to afford an easier comparison. See further explanation in the text.

dimensional phase has been detected experimentally [18]. It is also known experimentally that the inhomogeneity of the substrate plays a role in dilute ^{4}He adsorbed in this system [19].

According to the literature on classical noble gases [6], after the lower part of the grooves is filled, a three stripe ($3S$) phase is found. The trial function for this new phase was of the form $\Phi_J\Phi_1$ with $a_1 = 1.8$ Å^{-2}. x_{site} and y_{site} are a set of coordinates different for each atom: for the atoms in the lower part of the grooves, they are the same as the ones corresponding to a one-dimensional phase, while for ^{4}He on the sides, the minimum energy for the system was found for positions located at 9.5 Å from the center of the closest tube and 2.8 Å from the atom in the center of the groove. $b_1 = 0$. In all cases, the calculations were carried out with 90 particles distributed in three stripes along the z axis with simulation cell lengths adequate to get the inverse of the helium densities displayed in Fig. 3. The x axis is the inverse of the surface density. The area of the surface was taken to be as all the available space located at 9.5 Å from the center of any of the two tubes in the cell. According to the idea already indicated above, one expects the quasi-1D phase to be filled before the three stripes phase begins to do so. That is the reason why the Maxwell construction line (lower full line) is made from the minimum binding energy of the 1D phase to the maximum binding of the $3S$ one. This corresponds to densities of 1.4×10^{-2} Å^{-2} (1D) to 3.9×10^{-2} Å^{-2} (three stripes). The former density means that the average distance between helium atoms in the 1D phase at complete filling is 3.4 Å, the same result found experimentally for a bundle of (8,8) tubes [19]. The open circles in Fig. 3 are the results obtained for the maximum binding energies of an unstable zigzag phase [6] (two stripes of helium instead of one or three) on top of a groove.

The remaining part of the figure for volumes of 20 Å^2 and lower corresponds to a two-dimensional (2D) liquid phase. The trial function for this part was taken to be $\Phi_J\Phi_2$ with $a_2 = 1.8$ Å^{-2}. Φ_2 is a Gaussian in which the r coordinates are the distances of the ^{4}He atoms to the center axis of the nanotubes and $r_{\text{center}} = 9.5$ Å. We considered here a simulation cell that comprised three parallel nanotubes (length in the x axis of 34 Å) and 160 ^{4}He atoms. The length of the nanotubes in the z axis was changed to obtain the densities displayed in the figure. The upper full line corresponds to the Maxwell construction between this liquid phase and the three stripes one. The corresponding equilibrium densities are 6.2×10^{-2} Å^{-2} and 3.9×10^{-2} Å^{-2} (same as in the previous transition, indicating a very narrow stability range for the $3S$ phase). The only counterpart to this liquid monolayer is the one predicted at low coverages in the inner part of a (10,10) tube [30], since the first layer of helium of graphite is a solid [31].

The next step is to know what happens when still more helium is added. The possibilities are the formation of a solid monolayer and the promotion of the remaining helium to a second layer. All of them were explored. In Fig. 4, open squares represent the already discussed one-layer liquid, while the solid monolayer is indicated by full squares. Several solid structures were tried, the one with

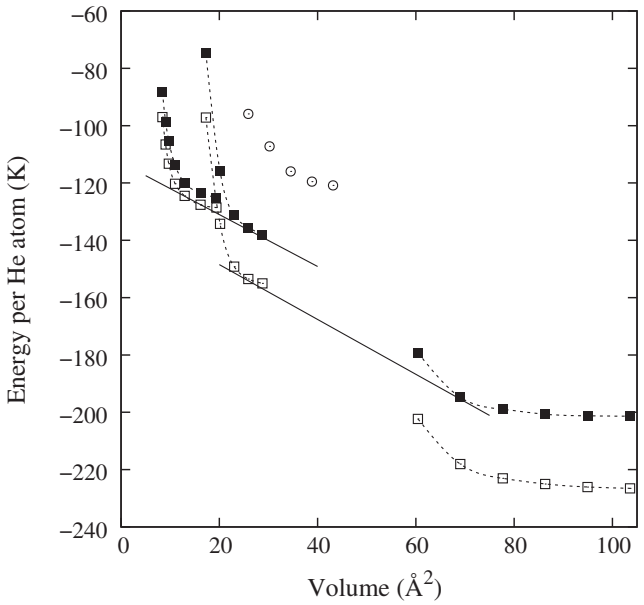

FIG. 3. Maxwell constructions for the different helium phases up to the monolayer limit. Lower set of curves, quasi-1D system; medium set, 3S phase; upper couple of curves, liquid monolayer. In all cases, full squares represent the results for the minimum binding energies per particle and open squares for the maximum ones. Dashed lines are guides to the eye. Open circles correspond to an unstable zigzag phase.

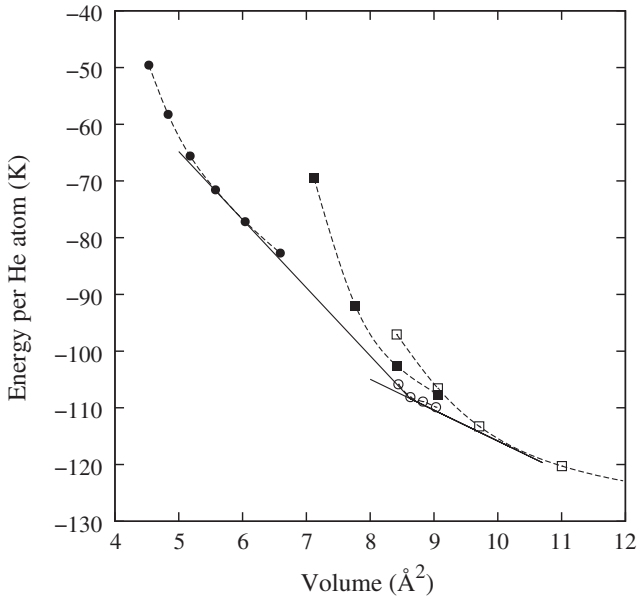

FIG. 4. Phases of helium at high densities: open squares, 2D liquid monolayer; full squares, 2D solid monolayer; open circles, 1D phase on top of a liquid; full circles, the two-layered phase discussed in the text.

minimum energy corresponding to what is called an eight-channel structure [6]. This means a layer formed by eight parallel rows of atoms on top of each tube, disposed in such a way as to form a triangularlike arrangement. The same simulation cell and number of atoms than in the case of the liquid were used. The trial function was of the form $\Phi_J\Phi_1$ with x_{site}, y_{site} and z_{site} the positions of atoms in the eight-channel structure just described. $a_1 = b_1 = 2.1$ Å^{-2}. The alternative to this solid monolayer is the formation on top of the liquid helium monolayer of the same structures than for the bare carbon nanotubes, i.e., a quasi 1D phase on the grooves, a three stripes one, and a liquid second layer. There was the additional problem of knowing what should be the surface density of the first layer of these structures, and if this first layer was a liquid or a solid one. Diffusion Monte Carlo calculations were performed for all the possibilities in the range of inverse densities displayed in Fig. 4 (lower than 10 Å^{-2}). The results for the minimum energy structures are actually shown in Fig. 4. Open circles correspond to a quasi-1D phase on top of a liquid monolayer of 0.103 Å^{-2}. The average distance of the ^{4}He atoms to each of the centers of both tubes was of 12.6 Å. The full circles are the energies per particle of a structure formed by an eight-channel solid monolayer in contact with the carbon nanotube and density 0.110 Å^{-2} and a liquid monolayer on top of it and whose atoms are located on average at a distance of the same 12.6 Å to the center of the closest tube. No other structure with lower energy in this density range was found. There is not, for instance, a double liquid layer nor a three stripes second-layer phase, nor a quasi-1D phase on top of a solid layer. From Fig. 4, we can say that the upper density for which the liquid monolayer is stable is 0.098 Å^2, density at which it is in equilibrium with a quasi-1D second-layer one of 0.116 Å^2. This 1D phase is also in equilibrium with a two layer one of density 0.18 Å^{-2}. The second-layer quasi 1D phase was found experimentally in the case of Ne [21], but to our knowledge has not been identified for helium. Nor is there any experimental indication of a solid + liquid phase at 0 K. The experimental results on the single monolayer seem to point to a solid, not to the liquid found here [19]. The difference could be due to the fact that the system is a different one [a bundle of (8,8) nanotubes instead of a (10,10) one] or to the fact that the simulation cell used here (only three tubes) could be too small.

Summarizing, we have performed a series of Diffusion Monte Carlo calculations on the adsorption of ^{4}He in the outside surface of a bundle of (10,10) nanotubes. We found the corrugation to be very important, and a series of phases ranging form a quasi-1D one to a two-layered one in which the closest helium sheet is a 2D triangular solid.

The Spanish Ministry of Education and Science (MEC) and the Junta de Andalucia are thanked for financial support under Grants FIS2006-02356 and P06-FQM-01869, respectively.

[1] S. Iijima, Nature (London) **354**, 56 (1991).
[2] M. M. Calbi, M. W. Cole, S. M. Gatica, M. J. Bojan, and G. Stan, Rev. Mod. Phys. **73**, 857 (2001).
[3] S. Talapatra, A. Z. Zambano, S. E. Weber, and A. D. Migone, Phys. Rev. Lett. **85**, 138 (2000).
[4] M. C. Gordillo, Phys. Rev. Lett. **96**, 216102 (2006).
[5] S. M. Gatica, M. J. Bojan, and G. Stan, J. Chem. Phys. **114**, 3765 (2001).
[6] M. M. Calbi, S. M. Gatica, M. J. Bojan, and M. W. Cole, J. Chem. Phys. **115**, 9975 (2001).
[7] N. M. Urban, S. M. Gatica, M. W. Cole and J. L. Riccardo, Phys. Rev. B **71**, 245410 (2005).
[8] M. Bienfait, P. Zeppenfeld, N. Dupont-Pavlovsky, M. Muris, M. R. Johnson, T. Wilson, M. DePies, and O. E. Vilches, Phys. Rev. B **70**, 035410 (2004).
[9] D. S. Rawat, L. Heroux, V. Krungleviciute, and A. D. Migone, Langmuir **22**, 234 (2006).
[10] Z. J. Jakubek and B. Simard, Langmuir **21**, 10730 (2005).
[11] L. Heroux, V. Krungleviciute, M. M. Calbi, and A. D. Migone, J. Phys. Chem. B **110**, 12597 (2006).
[12] W. Teizer, R. B. Hallock, E. Dujardin, and T. W. Ebbesen, Phys. Rev. Lett. **82**, 5305 (1999).
[13] W. Teizer, R. B. Hallock, E. Dujerdin, and T. W. Ebbesen, Phys. Rev. Lett. **84**, 1844 (2000).
[14] T. Wilson, A. Tyburski, M. R. DePies, O. E. Vilches, D. Becquet, and M. Bienfait, J. Low Temp. Phys. **126**, 403 (2002).
[15] S. Ramachandran, T. A. Wilson, D. Vandervelde, D. K. Holmes, and O. E. Vilches, J. Low Temp. Phys. **134**, 115 (2004).
[16] Y. H. Kahng, R. B. Hallock, E. Dujardin, and T. W. Ebbesen, J. Low Temp. Phys. **126**, 223 (2002).
[17] T. Wilson and O. E. Vilches, Physica B (Amsterdam) **329–333**, 278 (2003).
[18] J. C. Lasjaunias, K. Biljakovic, J. L. Sauvajol, and P. Monceau, Phys. Rev. Lett. **91**, 025901 (2003).
[19] J. V. Pearce, M. A. Adams, O. E. Vilches, M. R. Johnson, and H. R. Glyde, Phys. Rev. Lett. **95**, 185302 (2005).
[20] S. Ramachandran and O. E. Vilches, Phys. Rev. B **76**, 075404 (2007).
[21] S. Talapatra, V. Krungleviciute, and A. D. Migone, Phys. Rev. Lett. **89**, 246106 (2002).
[22] A. D. Lueking and M. W. Cole, Phys. Rev. B **75**, 195425 (2007).
[23] L. Firlej and B. Kuchta, Colloids Surfaces A: Physicochem. Eng. **241**, 149 (2004).
[24] A. Siber, Phys. Rev. B **66**, 205406 (2002).
[25] M. Aichinger, S. Kilic, E. Krotscheck, and L. Vranjes, Phys. Rev. B **70**, 155412 (2004).
[26] J. Boronat and J. Casulleras, Phys. Rev. B **49**, 8920 (1994).
[27] M. C. Gordillo, J. Boronat, and J. Casulleras, Phys. Rev. B **61**, R878 (2000).
[28] R. A. Aziz, F. R. W. McCourt, and C. C. K. Wong, Mol. Phys. **61**, 1487 (1987).
[29] G. Stan and M. W. Cole, Surf. Sci. **395**, 280 (1998).
[30] M. C. Gordillo, J. Boronat, and J. Casulleras, Phys. Rev. B **76**, 193402 (2007).
[31] M. E. Pierce, and E. Manousakis, Phys. Rev. B **62**, 5228 (2000).